Underwater Electric Field Measurement and Analysis

Ronnie Ross, Richard Oare, Michael Anderson, Eric Wolbrecht, John Canning, Jim Frenzel, Terry Soule, Juan Arias, Dean Edwards

Departments of Mechanical, Electrical, and Chemical Engineering
University of Idaho
Moscow, Idaho

***Abstract*—The University of Idaho (UI) is developing electromagnetic field sensor systems that are attachable to autonomous underwater vehicles with the intent of taking survey measurements in underwater ocean environments. This paper presents the testing of these sensors and compares measurements to predictions. Testing was conducted off the coast of Florida with a moving artificial electric field source and an electric field sensor equipped AUV. At the closest pass, the peak value of the AUV-acquired electric field was consistent with the predicted field of the artificial source when the accuracy of AUV position was known to within ~1 m.**

Keywords—AUV, Electric Field Ocean Measurements, Electric Field Modeling and Comparison

I. Introduction

Electromagnetic measurements in the ocean have been used for multiple applications including petroleum exploration [1], measuring sea-ice thickness [2], and locating targets in the water similarly to how some fish use electro-location [3, 4]. This research seeks to evaluate the effectiveness of using electric field sensors deployed by autonomous underwater vehicles (AUVs) to conduct electric field surveys in ocean environments.

Specifically, this research focused on developing and analyzing electric field sensors for performing ocean surveys. The electric field sensors were fixed to autonomous underwater vehicles (AUVs) and testing was conducted in both laboratory and field settings. Field tests were conducted at the South Florida Ocean Measurement Center (SFOMC) to obtain measurements of a moving electric field source.

Data from the field tests were analyzed to determine how effective the sensors were in measuring the source. These measurements were compared to theoretical models of the expected electric field. These comparisons were then used to analyze and identify where improvements could be made in the measurements.

II. Methods

A. Autonomous Underwater Vehicles (AUVs)

The AUVs used during these measurements, shown in Fig. 1, were a modified design based on work done by Virginia Polytechnic Institute [5]. The AUVs were 102 cm long and 10.2 cm in diameter; additional details of the AUV can be found in [6]. A separate, smaller PVC tube, which held batteries for the preamplifiers in the electric field sensors, was attached to the bottom of the AUV.

Fig. 1. University of Idaho autonomous underwater vehicle (AUV) with electric field sensor attached in normal operating configuration.

B. Electric Field Sensors

The electric field sensors used in these measurements were designed and constructed at UI. The sensors were made from a urethane elastomer compound which was poured into a 7.62 cm spherical mold. Each sensor contained six Ag/AgCl electrodes (three pairs) and a preamplifier for each pair. The preamplifier used was a low noise Texas Instruments INA 129 with a gain of 250. Previous electric field sensors had a 3.81 cm diameter and did not include the preamplifier inside the spherical probe [6]. Previously the preamplifier was held in a separate PVC tube which the electrodes were connected to through a fiberglass rod as shown in Fig. 1. The purpose of creating a larger diameter sensor was to move the preamplifier as close to the electrodes as possible to reduce the length of wires running along the AUV. The older design used smaller 2 mm diameter by 4 mm long electrodes. The newer 7.62 cm diameter probe used larger 12mm diameter electrodes with a 1 mm thickness. Digitization happened at a rate of 16.7 kHz with a 16-bit resolution over a ±1.25 V range [6]. Fig. 2 shows a representation of the sensor with the embedded electrodes and preamp.

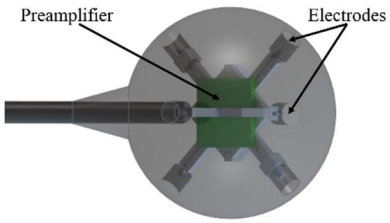

Fig. 2. Representation of electric field sensor probe with embedded electrodes and preamplifier

978-0-692-94690-9/$31.00 ©2017 MTS

The electric field sensor was attached to the AUV with a fiberglass rod that is shown in Fig. 1. The previous design held the preamplifier in the PVC tube shown in Fig. 1. The new design has the preamplifier in the probe with the electrodes as shown in Fig. 2.

C. Laboratory Testing

Testing was conducted to determine the noise floor of the electric field sensor. To mimic the expected ocean environment, a 473 L (125 gallon) 1.22 m by 0.91 m (4' by 3') plastic tank was filled with salt water at a concentration between 34 and 36 ppt. This salt water concentration is consistent with seawater found off the coast of South Florida. The tank was surrounded by a 3.05 m by 2.44 m by 2.44 m (10' by 8' by 8') faraday cage that was fabricated from aluminum mesh (1 mm by 1.5 mm holes) and a wooden frame. The purpose of the faraday cage was to mitigate external electromagnetic noise sources.

D. Field Testing

Testing was conducted at South Florida Ocean Measurement Facility (SFOMF). This site was 2.1 km offshore and the depth of the water was approximately 15.2 m (50'). The range was roughly 200 m by 200 m and the bottom consisted of sand and mud [6].

The testing range used a long-baseline (LBL) array of four deployed transponders fixed to the bottom of the seafloor for navigation purposes. An extended Kalman filter (EKF) was used to combine onboard sensor data with the acoustic ranges from the LBL array to estimate the position, speed, and heading of the AUV. The EKF also estimated ocean currents (North and East), through an observable combination of system and measurement models [6, 7].

A 7.6m long fiberglass source boat was outfitted with equipment to induce electric field signals in the water. This source used a 30 amp dc current to create a voltage potential across two electrodes attached to the bottom side of the hull, one at the stern-end and one at the bow-end.

During a typical test, the AUV and source boat would line up at opposite ends of the test range. The AUV would dive to a depth of 10 m and navigate along a straight line across the range while the source boat would follow the line in the opposite direction on the surface heading toward the AUV. The goal was to have the AUV and the source boat cross in the middle of the run so that the AUV could measure the source. The source boat induced an electric field which could be measured when the AUV was close to the source.

E. Electric Field Modeling

Determining the accuracy of our 7.62 cm diameter electric field sensor was an important part of the post analysis of our testing. The goal of this analysis was to determine the accuracy of our measurements by comparing them to theoretical models of the electric field in our offshore test environment.

The model consists of a single dipole in a three layered environment [8]. Fig. 3 shows a simplified representation of the environment [9]. The layers consist of the air, seawater, and seafloor. The source, q, and the measurement point, P, were located in the seawater. The model was broken down into two portions, the free space and the effects of the layers in addition to the free space. The images produced from the boundaries are denoted by a_n, a_0, b_n, b_0, c_n, c_0, d_n, and c_0.

The Z axis shows the height of each section of the environment. The top and bottom of the seawater layer were located at $z = 0$ and $z = -d$ respectively. The source electrodes

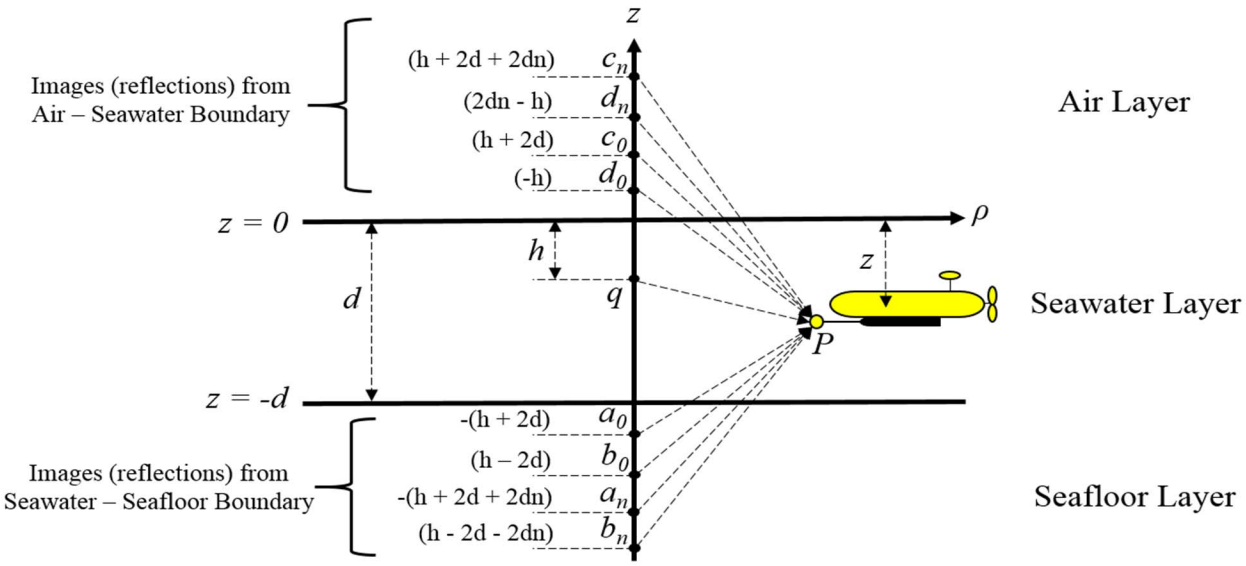

Fig. 3. Representation of the effects of the layers of the prediction model

were at the depth h, and ρ was the horizontal distance of the AUV to the source during the run. The following equations are used to calculate the total electric field voltage (V) [8]:

$$V = \frac{K_2}{r} + K_2 \sum_{n=0}^{\infty} \left[R_{23}^n R_{21}^n \left(\frac{R_{23}}{r_a} + \frac{R_{23}R_{21}}{r_b} + \frac{R_{23}R_{21}}{r_c} + \frac{R_{21}}{r_d} \right) \right], \quad (1)$$

$$K_2 = \frac{j\omega q}{4\pi Y_2}, \quad (2)$$

$$Y_i = \sigma_i + j\omega\epsilon_i, \quad (3)$$

$$E = -\nabla V. \quad (4)$$

Equation (4) shows the total voltage calculation which was used to calculate the free space combined with the boundary effects in an inertial frame. The first term of (1), before the summation term, is the free space electric field portion of the model. The summation term adds the effects of the boundary layers to the model. The layers were denoted as follows: $i = 1$ was the air, $i = 2$ was the seawater, and $i = 3$ was the seafloor. The admittance (Y_i) between boundaries (3) was determined by the conductivity (σ_i) and permittivity (ε_i) of each layer. For this application, $j\omega q$ was set equal to I, the current applied to the electrodes. In (2), the value for ω was near zero (ω = 0.00001) to replicate the DC measurements that were taken. The following equations break down the boundary layer effects [8]. The reflection coefficients, R_{21} and R_{23}, are denoted as

$$R_{21} = \frac{Y_2 - Y_1}{Y_2 + Y_1}, R_{23} = \frac{Y_2 - Y_3}{Y_2 + Y_3}, \quad (5)$$

and the distances to the images, r_a, r_b, r_c, and r_d, are given as

$$r_a = \sqrt{\rho^2 + (z + h + 2d(n+1))^2}, \quad (6)$$

$$r_b = \sqrt{\rho^2 + (z - h + 2d(n+1))^2}, \quad (7)$$

$$r_c = \sqrt{\rho^2 + (h - z + 2d(n+1))^2}, \quad (8)$$

$$r_d = \sqrt{\rho^2 + (2nd - z - h)^2}. \quad (9)$$

The properties of each layer were found in multiple sources. The conductivity of air used in this analysis was $\sigma_1 = 5.5e^{-15}$ Siemens per meter (S/m) [10]. The value of the conductivity of the seawater used in our computation was $\sigma_2 = 4.8$ S/m [11] and the conductivity of the seafloor used was $\sigma_3 = 5$ S/m [12]. The permittivity of these layers was found by multiplying the relative permittivity of the layer by the free space permittivity, $\varepsilon_1 = 8.85e^{-12}$ Farads per meter (F/m), which was the permittivity of the air. The relative permittivity of the seawater used was $\varepsilon_{r2} = 70$ [13] and the relative permittivity of the seafloor used was $\varepsilon_{r3} = 30$ [14]. These measurements could be potentially improved by taking actual measurements of the properties from the test range.

III. Results and Discussions

The results presented in this paper focus on determining the effectiveness of our electric field sensors equipped to AUVs to accurately measure electric fields in ocean environments. The comparison of the electric field measurements to theoretical models is also presented.

A. Noise Floor of Electric Field Sensor

Laboratory testing was conducted to determine the noise floor of the electric field sensors. The electric field sensor was attached to an AUV and placed in the tank. The AUV was then strapped on a PVC frame to hold it in place during testing. During testing, the AUV was powered as if it was in normal operation with the exception of the motor for the propeller not being run.

Fig. 4 shows the noise floor of one of our electric field sensors in a controlled laboratory environment. The important information from this was that the overall RMS levels of the electrode pairs was 1 μV/m over the 0.02 Hz to 20 Hz bandwidth. The data was low-pass filtered at 20 Hz.

B. Field Tests and Model Comparison

Two days of testing were conducted off the shore of South Florida at SFOMF. The results presented here are from one of the optimal runs during these tests. Fig. 5 shows the position and depth of the AUV during the run.

The left plot of Fig. 5 shows the path of the AUV and the surface boat with the electric field source during the run. The position of the GPS tracks of each electrode from the source boat are the red and blue lines. The AUV path is shown as the black line. The arrows show which end of the range the vehicles start and which direction they moved during the run. The right plot of Fig. 5 shows the depth of the AUV as a black line. The blue line shows the distance between the AUV and the source boat. The closest pass of the AUV and the source

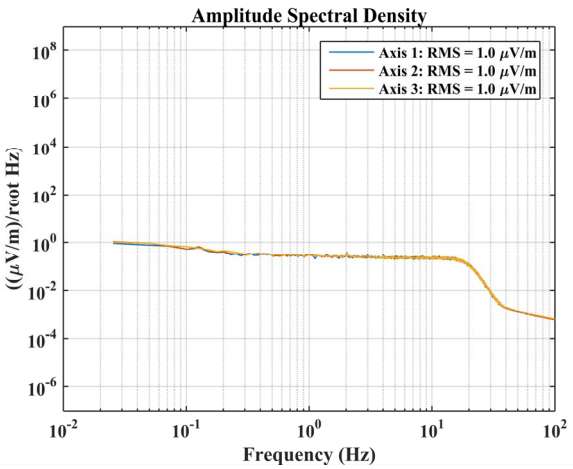

Fig. 4. Amplitude spectral density of noise floor measurements in a controlled laboratory environment.

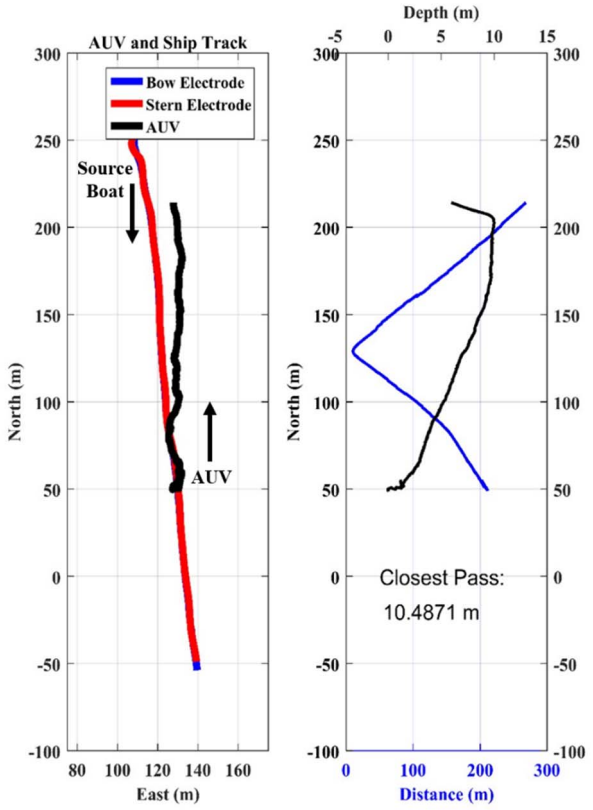

Fig. 5. LEFT: North and East position of the AUV (black) and source boat (red and blue) during Florida offshore field testing. RIGHT: Depth of AUV (black) during the same mission as a function of North position. Distance from the AUV to the source boat is also shown (blue).

during this run was ~10.5 m. This distance was the total distance between the AUV and the source, including the depth.

Fig. 6 shows the evaluation of the magnitude of the measured electric field during the same mission shown in Fig. 5. The magnitude of the measured electric field is shown in blue. The free space component of the predicted electric field is the red line and the yellow line shows the prediction including the effects of the layers. These models take into account the position of the AUV and the position of the source to calculate the prediction of the electric field.

The magnitude of the measured electric field had a peak value of just under 7,000 µV/m and lies between the predictions of the electric field. The peak values of the free space portion and the addition of the layered effects were 2,000 µV/m and just under 10,000 µV/m respectively. This shows that the measured value lies between where the theoretical models predict. This verified the plausibility of our measurement system.

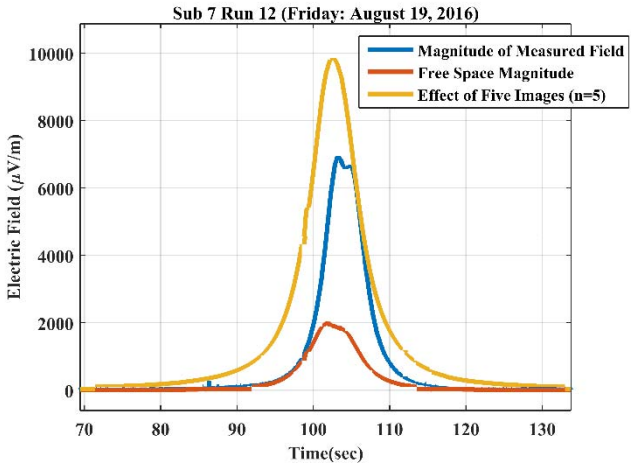

Fig. 6. Magnitude of the electric field measurement and the prediction models based on the position of the AUV during the course of the run.

These results led us to evaluate areas that could be sources of error which if improved could lead to more accurate electric field measurements. It was simple to change various parameters in the theoretical prediction and examine how they affected the prediction of the electric field magnitude.

The main variable that was examined was the navigation data of the AUV. The AUV position was only known to within a couple of meters at the time of this testing. To investigate the impact of this uncertainty, each coordinate of the position data was varied by a meter; i.e. a meter was added or subtracted from the north, east, and depth coordinates. The position of the AUV, (*x, y, z*), was varied to both (*x + 1, y + 1, z + 1*) and (*x - 1, y - 1, z - 1*) which corresponds to the free space plus or minus one meter and the layered effects plus or minus one meter on Fig. 7. Fig. 7 shows the corresponding plot of the magnitude of the electric field with these position changes compared to the original computation of the model.

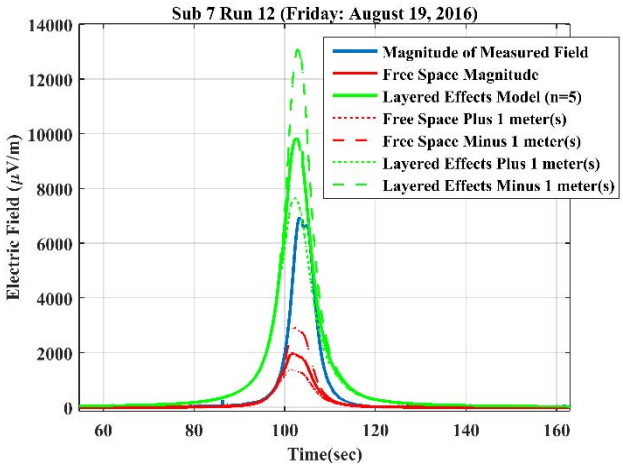

Fig. 7. Sensitivity of the magnitude of the electric field predictions due to uncertainty in the AUV position.

The solid green and solid red lines show the computed models without the addition or subtraction of a meter from the AUV position. The dashed lines show what the predicted model would be if a meter was subtracted from each position coordinate. The dotted lines show what would happen if a meter was added to each coordinate. The largest effect comes from the depth changing. The dashed line predicts a stronger measurement which physically would make sense because the AUV would then be a meter closer to the source. The opposite holds for the dotted line; it predicts a weaker magnitude. The model, including the layered effects, that was based on the actual position of the AUV predicts a peak value of just under 10,000 μV/m for the electric field magnitude. When the AUV was theoretically moved closer to the source, the peak value increased to 13,000 μV/m, and when the AUV was theoretically moved further away, the peak value decreased to 7,700 μV/m. This analysis begins to give bounds on the predicted electric field based on the accuracy of the AUV position. A large portion of the difference between the actual measurement and the predicted model could be explained by the prevalent uncertainty in AUV position.

IV. Conclusions and Future Work

This research has demonstrated the capability of AUVs to measure the electric field of a moving source in the ocean. Experimental results and data analysis have shown that the measurements of electric fields were within the theoretical range of the prediction models. Comparing the measurements to the prediction models showed that there are improvements that can be made to the AUV position accuracy which could lead to increased accuracy in the electric field measurement.

Acknowledgment

This work was supported by the U.S. Office of Naval Research (N00014-14-1-0662 and N00014-16-1-3103).

References

[1] S. C. Constable, A. S. Orange, G. M. Hoversten, and H. F. Morrison, "Marine magnetotellurics for petroleum exploration Part I: A sea-floor equipment system," *Geophysics,* vol. 63, no. 3, pp. 816-825, 1998.

[2] J. E. Reid, A. P. Worby, J. Vrbancich, and A. I. Munro, "Shipborne electromagnetic measurements of Antarctic sea-ice thickness," *Geophysics,* vol. 68, no. 5, pp. 1537-1546, 2003.

[3] G. Schultz, J. Miller, F. Shubitidze, and R. Evans, "Underwater controlled source electromagnetic sensing: Locating and characterizing compact seabed targets," in *Oceans, 2012*, 2012, pp. 1-9: IEEE.

[4] Y. Bai, J. B. Snyder, M. Peshkin, and M. A. MacIver, "Finding and identifying simple objects underwater with active electrosense," *The International Journal of Robotics Research,* vol. 34, no. 10, pp. 1255-1277, 2015.

[5] D. J. Stilwell, A. S. Gadre, C. A. Sylvester, and C. J. Cannell, "Design elements of a small low-cost autonomous underwater vehicle for field experiments in multi-vehicle coordination," in *Autonomous Underwater Vehicles, 2004 IEEE/OES*, 2004, pp. 1-6: IEEE.

[6] S. R. Qualls *et al.*, "Underwater electric potential measurements using auvs," in *OCEANS'15 MTS/IEEE Washington*, 2015, pp. 1-4: IEEE.

[7] J. Osborn, "AUV State Estimation and Control in the Presence of Ocean Currents," ed, 2016, p. 60.

[8] R. T. Rebich, J. L. Young, C. L. Wagner, and R. G. Olsen, "Comparison of the up-over-down approximation with the quasi-electrostatic approximation for ELF fields in layered media," in *Antennas and Propagation (APSURSI), 2011 IEEE International Symposium on*, 2011, pp. 2371-2374: IEEE.

[9] R. Ross, "Measurement and Analysis of Electric Fields in Ocean Environments," M.S. M.E., College of Engineering, University of Idaho, 2017.

[10] S. Pawar, P. Murugavel, and D. Lal, "Effect of relative humidity and sea level pressure on electrical conductivity of air over Indian Ocean," *Journal of Geophysical Research: Atmospheres,* vol. 114, no. D2, 2009.

[11] R. Cox, M. McCartney, and F. Culkin, "The specific gravity/salinity/temperature relationship in natural sea water," in *Deep Sea Research and Oceanographic Abstracts*, 1970, vol. 17, no. 4, pp. 679-689: Elsevier.

[12] R. E. Boyce, "Electrical resistivity of modern marine sediments from the Bering Sea," *Journal of Geophysical Research,* vol. 73, no. 14, pp. 4759-4766, 1968.

[13] W. Ellison *et al.*, "New permittivity measurements of seawater," *Radio science,* vol. 33, no. 3, pp. 639-648, 1998.

[14] S. Arcone, S. Grant, G. Boitnott, and B. Bostick, "Complex permittivity and clay mineralogy of grain-size fractions in a wet silt soil," *Geophysics,* vol. 73, no. 3, pp. J1-J13, 2008.